Nexo Revista Científica
Vol. 27, No. 02, pp. 115-124 / December 2014

ISSN: 1818-6742 print / 1995-9516 online
DOI: 10.5377/nexo.v27i2.1947

Simulation of a continuous plug-flow fluidised bed dryer for rough rice†

Apolinar Picado[1,2,*], Rafael Gamero[3]

[1]Department of Chemical Enginering and Technology, KTH Royal Institute of Technology
SE-100 44 Stockholm, Sweden
[2]Department of Engineering and Computer Science, Keiser University Latin American Campus
San Marcos 45000, Nicaragua
[3]Facultad de Ingeniería Química, Universidad Nacional de Ingeniería (UNI)
PO Box 5595, Managua, Nicaragua

(recibido/received: 02-Jun-2014; aceptado/accepted: 08-Nov-2014)

ABSTRACT

In this study, a mathematical model to simulate the drying of rough rice in a continuous plug-flow fluidised bed dryer is presented. Equipment and material models were applied to describe the process. The equipment model was based on the differential equations obtained by applying mass and energy balances to each element of the dryer. Concerning the material model, mass and heat transfer rates in a single isolated particle were considered. Mass and heat transfer within the particles was described by analytical solutions with constant effective transport coefficients. To simulate the dryer, the material model was implemented in the equipment model in order to describe the whole process. Calculation results were verified by comparison with experimental data from the literature. There was very good agreement between experimental data and simulation. The effects of gas temperature and velocity, particle diameter, dry solid flow and solid temperature on the drying process were investigated. It was found that the changes in gas velocity, dry solids flow and solid temperature had essentially no effect on drying behaviour.

Keywords: Plug-flow; Fluidised bed dryer; Modelling; Rough rice

RESUMEN

En este estudio, se presenta un modelo matemático para simular el secado de arroz con cáscara en un secador continuo de lecho fluidizado con flujo pistón. Para describir el proceso se aplicó un modelo del equipo y un modelo del material. El modelo del equipo se basó en las ecuaciones diferenciales obtenidas por la aplicación de balances de masa y energía a cada elemento del secador. En relación al modelo del material, se consideraron velocidades de transferencia de masa y calor en una partícula aislada. La transferencia de masa y calor dentro de las partículas fue descrita por soluciones analíticas con coeficientes efectivos de transporte constantes. Para simular el secador, el modelo del material fue implementado en el modelo del equipo con el fin de describir el proceso completo. Los resultados de la simulación fueron verificados por medio de la comparación con datos experimentales de la literatura. Se comprobó que existe una alta concordancia entre los datos experimentales y la simulación. Se investigaron los efectos de la temperatura y velocidad del gas, diámetro de partícula, flujo de solidos secos y temperatura del solido sobre el proceso de secado. Se encontró que los cambios en la velocidad del gas, flujo de solidos secos y temperatura del solido no tuvieron efecto esencialmente sobre el comportamiento del secado.

Palabras clave: Flujo pistón; Secador de lecho fluidizado; Modelación; Arroz con cáscara

†Dedicated to Professor Joaquín Martínez (KTH/Sweden) on the occasion of his 65th birthday.

*Corresponding author. Tel.: +46 8 790 6570.
E-mail address: picado@kth.se (A. Picado).

1. Introduction

Rough rice (*Oryza sativa* L.) is one of the most consumed crops as it provides staple food for more than half of the world population. Moisture content is one of the most important factors influencing the quality of rough rice during storage and it remains at high level during the harvest 20-30 % (dry basis) and must be reduced with an appropriate drying process. The drying characteristics of rough rice have been studied by many researchers and various models for the prediction of drying rate have been performed with moderate success (Hacıhafızoglu *et al*., 2008).

Fluidised bed drying is an extensively employed drying method for wet particulates and granular materials that can be fluidised; and even slurries, pastes and suspensions that can be fluidised in beds of inert solids. The principal advantages of fluidised bed drying emerge from good solids mixing, high mass and heat transfer rates and easy material transport, which shorten drying time and prevent damage of thermo-sensitive materials (Park *et al*., 2006).

Most of the existing models of plug-flow fluidised bed dryers are based on knowledge of the interaction between the solid and gas phases. For instance, Khanali *et al*. (2013) have presented a model for a plug-flow fluidised bed dryer under steady-state conditions based on partial differential equations. A very satisfactory agreement between the theoretical and experimental data was achieved. Additionally, Khanali *et al*. (2014) have also presented a model for a plug-flow fluidised bed dryer under dynamic conditions resulted from the transient of inlet dry solids mass flow rate. The model equations were solved numerically using the finite difference method. A very satisfactory agreement between simulated and measured results was achieved. Bizmark *et al*. (2010) reported a sequential method to model a continuous plug-flow fluidised bed dryer, which is based on dividing the dryer into sections in series with ideal mixing for both solid and gas phases in each section. It was shown that the model fitted the experimental data satisfactorily. Daud (2007) has used the steady-state cross-flow model for estimating the profiles for solids and air moisture contents and temperatures in a continuous fluidised bed dryer. These profiles were shown to be dependent on the gas-solid flow ratio.

Izadifar and Mowla (2003) developed a mathematical model to simulate the drying of moist paddy rice in a cross-flow continuous fluidised bed dryer, applying momentum, mass and energy balances to each element of the dryer. Also, the non-ideal flow of solids in plug-flow fluidised dryers has been modelled as several continuous back-mixed fluidised bed dryers connected in several ways (Wanjari *et al*., 2006; Baker *et al*., 2010). The problem with this type of model is the difficulty of estimating a sufficient number of completely mixed dryers for any particular dryer a priori. It could only be determined by analysis of pilot-plant data (Daud, 2008).

Building on the results of an earlier study (Picado and Martinez, 2012), the present work was aimed to study the mathematical modelling and simulation of a continuous plug-flow fluidised bed dryer for rough rice. This was performed by incorporating a material model for a single wet grain, amenable to be solved analytically, in an incremental equipment model assuming plug-flow of the solids with gas cross-flow. The validity of the model was tested by comparison of model predictions with experimental data from the literature.

2. Description of the model

A schematic description of the continuous plug-flow fluidised bed dryer is shown in Fig. 1. Rough rice particles enter the dryer by a helical feeder and are fluidised smoothly by the upward flow of gas, normally air coming from the bottom of the bed through a gas distributor. An effective mixing of the rough rice particles takes place and a homogeneous material at a vertical cross-section of the dryer is usually obtained. Due to fluidisation and the slope of the dryer, rough rice particles move forward along the dryer and a partially dry product exits from the end.

The details of the model have been presented elsewhere (Picado and Martínez, 2012) and only the essentials are outlined here.

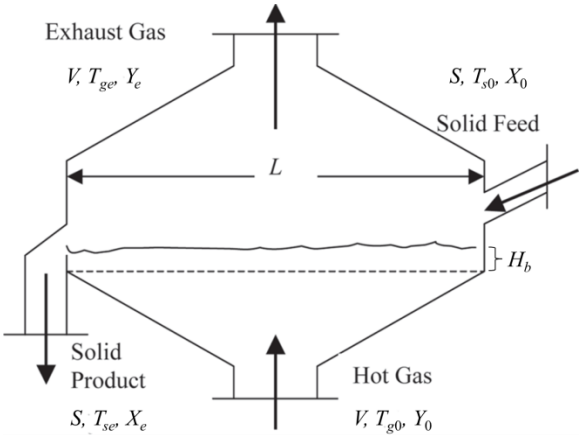

Fig. 1 A plug-flow fluidised bed dryer.

The following assumptions are introduced to simplify the complex characteristics of the process in the dryer:

- Rough rice is a spherical grain, isotropic, uniform in size and homogenous.
- The grain is perfectly well mixed in the vertical direction.
- Shrinkage of the grain during drying is negligible.
- Physical properties of the dry grain remain constant with time.
- The inlet distribution of the moisture content and temperature is uniform.
- Heat and mass transfer inside the grain takes place only in the radial direction.
- Moisture at the grain surface is in equilibrium with the gas humidity.
- The dryer is perfectly insulated.

2.1. Mass and energy balances

In the analysis of the dryer, it was assumed that the bed of particles was moving forward at a uniform velocity and that the dryer had been operating for long enough to ensure that steady-state conditions were reached. A moisture balance applied to the differential volume element shown in Fig. 2 yields:

$$F_s \frac{dX_b}{dz} = -a_s M G_g \tag{1}$$

where X is the solid moisture content on a dry basis, M is the molecular weight of the moisture, a_s is the specific evaporation area per unit bed volume, G_g is the molar evaporation flux, F is a mass flow per cross section in the direction of the flow and z is the distance along the bed from the solids inlet. The subscripts s and b denote solid and bed, respectively.

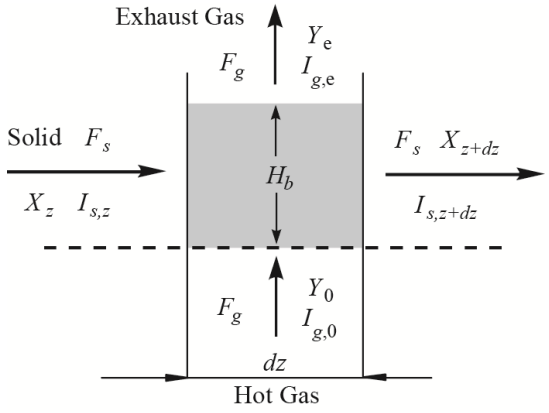

Fig. 2 Scheme of a differential dryer element.

Because all of the evaporated liquid goes to the gas, the following equation gives the change in gas humidity:

$$F_g \, dY = -F_s H_b \frac{dX_b}{dz} \tag{2}$$

where Y is the gas humidity on a dry basis and H_b is the bed height. The subscript g denotes gas. The bed height is calculated as

$$H_b = \frac{S}{v\rho_p(1-\varepsilon_p)(1-\varepsilon_b)B} \tag{3}$$

where S is the flow of dry solids, v is forward bed velocity, ρ is the density, ε is the porosity and B is the dryer width. The subscript p denotes particle. Because heat losses in the dryer are neglected, the energy balance over the same differential volume element becomes

$$dI_g = -H_b \frac{F_s}{F_g} \frac{dI_s}{dz} \tag{4}$$

where I is the enthalpy of the phases per unit mass on a dry basis. To integrate Eq. (1) to determine the changes in mean moisture content of the grain along the dryer, in addition inlet conditions, the evaporation flux must be provided. This flux depends on the temperature and moisture content at the surface of the particles. This information can be obtained by analysing what happens with a single particle moving along the dryer.

2.2. Drying of a single particle

The drying of a single wet particle into an inert gas is schematically described in Fig. 3. During the drying process, the moisture migrates from the centre of the solid particle towards the surface, where it evaporates. Migration occurs due to the moisture gradient in the solid particle by several mechanisms: molecular diffusion (liquid and vapour), capillary flow, Knudsen diffusion, surface diffusion, or combinations of the foregoing mechanisms. Usually, all of these mechanisms are lumped into an effective liquid transport mechanism using Fick's law for mass flux, which seems to describe the experimental data fairly well (Mujumdar, 2007; Saravacos and Maroulis, 2001).

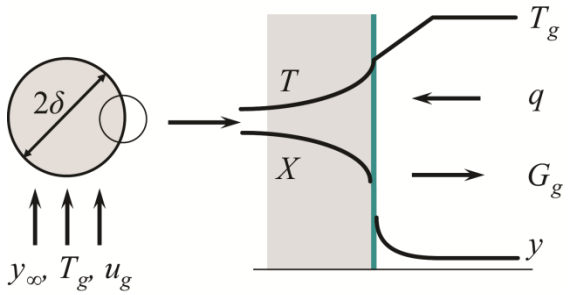

Fig. 3 Schematic of drying of a single particle into a gas.

Based on the assumptions outlined above, a set of space-averaged governing equations can be written for the particle. The longitudinal location of a particle in the dryer is related to the residence time (t) by the linear velocity of the bed (v). This allows one to track the changes in moisture content and temperature of particles as functions of distance along the bed (z). By introducing this change in variables, the diffusion equation for the spherical particle is

$$v\frac{\partial X}{\partial z} = D_{eff}\left(\frac{\partial^2 X}{\partial r^2} + \frac{2}{r}\frac{\partial X}{\partial r}\right) \tag{5}$$

where r is the radial coordinate and D_{eff} is the effective mass transport coefficient, which is estimated using an equation reported by Steffe and Singh (1982).

If conduction is the only mechanism for heat transfer within the particle, the corresponding equation to describe temperature changes is the conduction equation:

$$v\frac{\partial T}{\partial z} = D_h\left(\frac{\partial^2 T}{\partial r^2} + \frac{2}{r}\frac{\partial T}{\partial r}\right) \tag{6}$$

where D_h is the thermal diffusivity of the wet grain and T is the temperature.

Equations (5) and (6) represent a system of partial differential equations with the following inlet and boundary conditions:

At $z = 0$ and $0 \le r \le \delta$,

$$X = X_0\ \{r\}; \qquad T = T_0\ \{r\} \tag{7}$$

At $z > 0$ and $r = 0$,

$$\frac{\partial X}{\partial r} = 0\,; \qquad \frac{\partial T}{\partial r} = 0 \tag{8}$$

At $z > 0$ and $r = \delta$,

$$\begin{aligned} -\rho_p D_{eff}\frac{\partial X}{\partial r} &= M G_g \\ -k_{eff}\frac{\partial T}{\partial r} &= h(T - T_{g,\infty}) + \lambda G_g \end{aligned} \tag{9}$$

where δ is the particle radius, k is the thermal conductivity of the wet solid and λ is the latent heat of vaporisation. The subscripts 0, *eff* and ∞

denote inlet, effective value and gas bulk, respectively. Effective physical properties can be estimated by averaging the corresponding properties of the solid and moisture.

2.3. Mass and heat transfer rates

At the interphase, the evaporation flux is simply calculated as

$$G_g = k_m\,(y_\delta - y_\infty) \tag{10}$$

where k_m is the mass transfer coefficient, and y_δ and y_∞ are the vapour molar fractions at the gas-wet solid interface and in the gas bulk, respectively. In a hygroscopic material, the vapour pressure at the surface will be lower than the saturated value. This is accounted for by introducing a sorption isotherm that relates the equilibrium vapour pressure at the solid surface to the saturated value. In the present study, an empirical equation reported by Pfost *et al*. (1976) is used to correlate experimental equilibrium data. This information is inserted into Eq. (10), where y_δ is given by ratio between the partial pressure of water vapour and the total pressure. The convective heat flux can be calculated as:

$$q = h\,(T_{g,\infty} - T_\delta) \tag{11}$$

where h is the heat transfer coefficient between the drying gas and particle, and is estimated using a correlation reported by Yang (2003). The mass transfer coefficient can be calculated from the heat transfer coefficient by applying Lewis relationship because the Prandlt and Schmidt numbers are almost equal for mixtures of water vapour and air (Mujumdar, 2007).

2.4. Solution of the model

Equation (1) is a nonlinear ordinary differential equation that can be solved numerically using Euler's or any other standard method. Mass and heat transfer rates are required in the mass and energy balances along the dryer. The simultaneous solution of Eqs. (5) and (6), subjected to inlet and boundary conditions (7) through (9), provides the moisture content and temperature gradients in the particle as well as mass and heat transfer rates at the particle surface. By assuming constant transport coefficients as well as constant mass and heat transfer rates in each integration step of Eq. (1), Eqs. (5) and (6) can be solved analytically. In dimensionless form, the solution of Eq. (5) is

$$u = 2\sum_{k=1}^{\infty} \exp(-D_d\,\nu_{m,k}^2\,\tau)\left(\frac{\nu_{m,k}^2 + (\phi-1)^2}{\nu_{m,k}^2 + \phi(\phi-1)}\right) \times \left\{\int_0^1 u_0(\zeta)\sin(\nu_{m,k}\,\zeta)\,d\zeta\right\}\sin(\nu_{m,k}\,\zeta) \tag{12}$$

where $\pm\,\nu_{m,k}$, $k = 1, 2,\ldots$ are the roots of

$$\tan(\nu_{m,k}) = (1-\phi)^{-1}\nu_{m,k} \tag{13}$$

Finally, the dimensionless moisture content, u, is transformed back to obtain the moisture content in the particle:

$$X = \phi^{-1}\left(\frac{u}{\zeta} - y_b\right) \tag{14}$$

Analogously, the solution of Eq. (6) is

$$\Theta = 2\sum_{k=1}^{\infty} \exp(-\kappa\,\nu_{h,k}^2\,\tau)\left(\frac{\nu_{h,k}^2 + (a-1)^2}{\nu_{h,k}^2 + a\,(a-1)}\right) \times \left\{\int_0^1 \Theta_0(\zeta)\sin(\nu_{h,k}\,\zeta)\,d\zeta\right\}\sin(\nu_{h,k}\,\zeta) \tag{15}$$

where $\pm\,\nu_{h,k}$, $k = 1, 2,\ldots$ are the roots of

$$\tan(\nu_{h,k}) = (1-a)^{-1}\nu_{h,k} \tag{16}$$

Substitution back to temperature:

$$T = T_g - \frac{(T_g - T_0)}{a}\left(\frac{\Theta}{\zeta} - b\right) \tag{17}$$

The details of the analytical solutions and dimensionless variables as well as other parameters of the solutions can be found in Picado and Martínez (2012). Because the

conditions change along the dryer, the analytical solutions are applied to an interval *dz*, with inlet conditions and averaged transport coefficients corresponding to the outlet conditions of the previous step. As the integration of Eq. (1) proceeds, the procedure is repeated step by step. The outlet composition of the gas at each step *dz* is calculated using Eq. (2). Then the energy balance, Eq. (4), allows for the calculation of the exhaust gas enthalpy using the mean particle temperature to calculate the outlet enthalpy of the wet solids. Because the gas enthalpy is a function of gas composition and temperature, the outlet gas temperature can be calculated from a nonlinear equation that relates gas temperature with the gas enthalpy. Integration proceeds in this way until the dryer exit is reached.

3. Results and discussion

3.1. Model validation

In order to investigate the validity of the model predictions, the theoretical results were compared with pilot-scale experimental data from the literature. The material under consideration was long-grain rough rice from Mazandaran, Iran. The experimental fluidised bed dryer consisted of a chamber with a rectangular cross section for the gas flow of 1 m × 0.08 m and a height of 0.4 m. Details of the experimental procedure can be found elsewhere (Khanali *et al*., 2013). The experimental data sets were either cited directly from tables or read (digitised) from experimental points on figures in Khanali *et al*. (2013). The basic physical properties of rough rice used in the simulation are summarised in Table 1.

Table 1 Physical properties of rough rice (Khanali *et al*., 2013).

Particle diameter (m)	3.43×10^{-3}
Particle density (kg/m^3)	857
Particle porosity	0.48
Specific heat (J/kg K)	1,110
Thermal conductivity (W/m K)	0.10

Figures 4 and 5 show a comparison between the mean moisture content and mean solid temperature predicted by the mathematical model and experimental data for the same operating conditions. Both cases exhibited a very good agreement with the experimental data. As can be seen in the figures, the predicted and experimental moisture contents exhibited a smooth exponential decay curve over the whole length of the dryer that characterises the drying in the falling rate period for hygroscopic materials. Air drying of many food and agricultural products, such as rough rice, displays no constant rate period and the internal resistance to moisture transfer controls the drying process (Mujumdar, 2007). The temperature of the solids increases within a short distance from the solid inlet port and approaches a temperature nearly the same as the inlet gas temperature, remaining nearly constant until it exits the dryer. In the initial stages of drying, the mathematical model overestimates the solid temperatures of rough rice. However, it is difficult to discern whether it is due to limitation of the model or uncertainties in the experimental data. Due to the complex flow pattern in the dryer it is not always possible to obtain representative samples. Additionally, measuring the exact particle temperature is a difficult task. The trends of the experimental data and the simulation results of solid temperature are not in accordance with previous works in continuous plug-flow fluidised bed dryers, but it should be noted that any experimental support for the simulation results has not been provided in these works (Izadifar and Mowla, 2003; Wanjari *et al*., 2006; Baker *et al*., 2010). Parity plots of the measured and calculated values of mean solid moisture content and mean solid temperature for both continuous plug-flow fluidised bed drying experiments are shown in Fig. 6. The computed and measured values agree very well for both drying experiments. It can be observed that the present model correctly describes the drying process with good accuracy.

3.2. Effects of operational conditions on drying kinetics

Because knowledge of the parameters that significantly impact drying behaviour is useful in designing dryers, simulations were extended to predict the effects of operating parameters.

The basic data used in the simulations that follow were the same as those in Fig. 4. In all cases, a ± 15% variation in the operating parameters was applied.

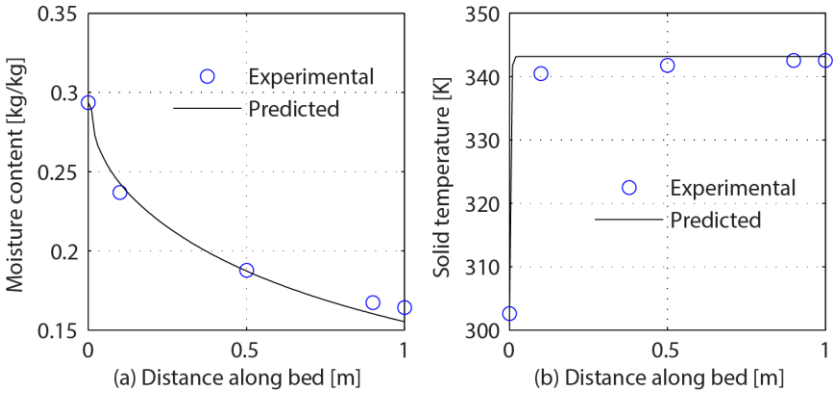

Fig. 4 Comparison between experimental and predicted moisture content and solid temperature along the bed length. u_g = 2.50 m/s, $T_{g,0}$ = 343.15 K, Y_0 = 0.0094 kg/kg, S = 8.10 kg/h, X_0 = 0.2936 kg/kg, $Ts_{,0}$ = 302.65 K, v = 0.0013 m/s.

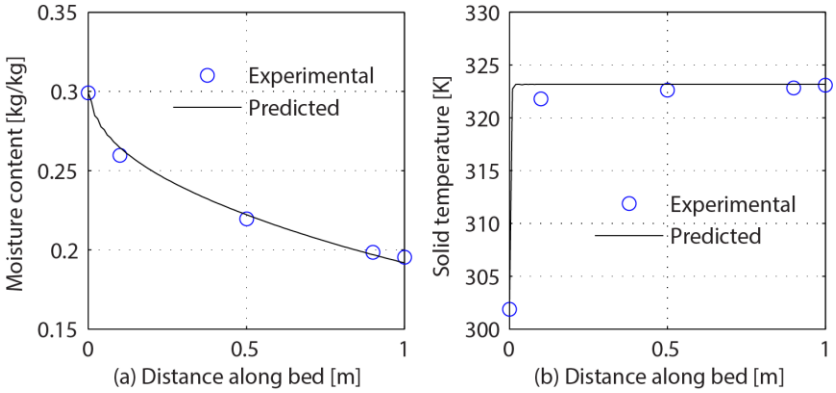

Fig. 5 Comparison between experimental and predicted moisture content and solid temperature along the bed length. u_g = 2.50 m/s, $T_{g,0}$ = 323.15 K, Y_0 = 0.0141 kg/kg, S = 2.76 kg/h, X_0 = 0.2990 kg/kg, $T_{s,0}$ = 301.90 K, v = 0.0011 m/s.

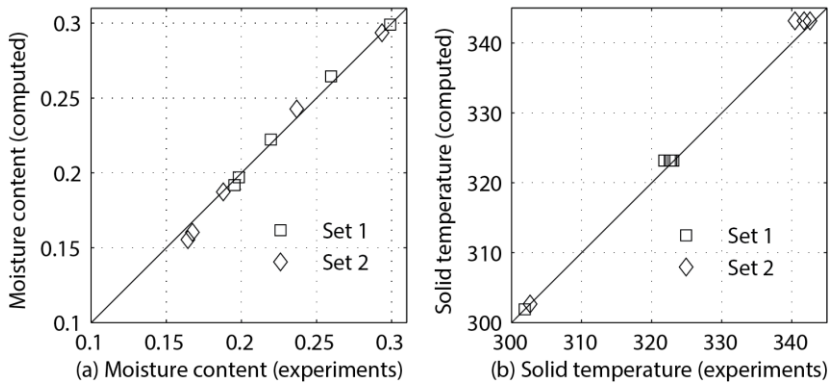

Fig. 6 Comparison of computed and experimental values of: (a) solid moisture content and (b) solid temperature.

Effect of inlet gas temperature

Figure 7 depicts the effect of inlet gas temperature (60 to 80ºC) on moisture content and solid temperature profiles along the length of the dryer. The drying rate was found to increase and hence the constant rate period ends earlier. As the temperature of inlet gas increases, the particle dries to lower final moisture content; thus, the value of the final moisture content decreases with an increase in the inlet gas temperature and the solid should attain the final equilibrium moisture content much earlier (see Fig. 7a). This effect can also be observed from the temperature profile. A higher inlet gas temperature induces faster heat and mass transfer rates because the driving force (i.e., temperature gradient) increases with inlet gas temperature.

Additionally, the resistance against heat transfer inside the solid is much lower than the resistance against mass transfer inside the solid. This means that convection heat not used to evaporate water is used to increase the solid temperature (see Fig. 7b), which in turn leads to higher coefficient of moisture transfer inside the solid and higher partial vapour pressure at the solid-gas interphase and hence to higher drying rates. The constant final solid temperature increased characteristically with an increase in inlet gas temperature as shown in Fig. 7b.

Effect of particle size

Figure 8 illustrates the effect of particle diameter on the drying process. As shown in Fig. 8a, increasing the particle diameter reduces the evaporation of the solid moisture content. Larger particles contain much longer diffusional paths within the solid, thus increasing internal resistance against mass transfer. Figure 8b shows that changes in particle diameter had very little effect on the solid temperature along the length of the dryer. Slight changes in solid temperature can be seen in the vicinity of the solid inlet port.

Under the conditions of the present simulations, it was found that the changes in gas velocity, dry solid flow and solid temperature had essentially no effect on drying behaviour (results not shown). A similar result has also been reported by Bizmark *et al*. (2010) and Khanali *et al*. (2013).

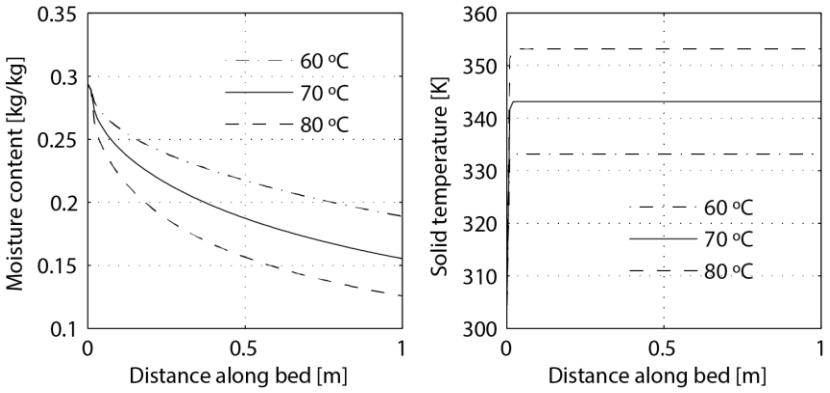

Fig. 7 Effect of gas temperature on drying behaviour. u_g = 2.50 m/s, Y_0 = 0.0094 kg/kg, S = 8.10 kg/h, X_0 = 0.2936 kg/kg, $T_{s,0}$ = 302.65 K, v = 0.0013 m/s.

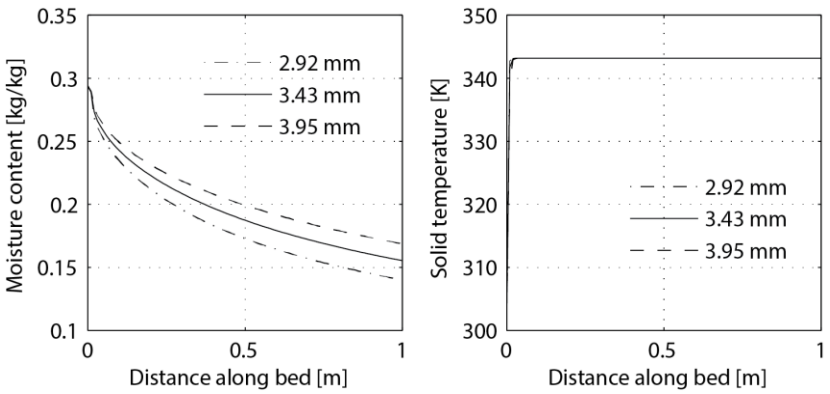

Fig. 8 Effect of particle size on drying behaviour. u_g = 2.50 m/s, $T_{g,0}$ = 343.15 K, Y_0 = 0.0094 kg/kg, S = 8.10 kg/h, X_0 = 0.2936 kg/kg, $T_{s,0}$ = 302.65 K, v = 0.0013 m/s.

4. Conclusions

In this work, a continuous plug-flow fluidised bed dryer model has been presented and validated. The predicted moisture content and temperature using the proposed model showed very good agreement with experimental data. Simulations based on this model were conducted to study the effects of operating parameters such as gas temperature, gas velocity, particle size, dry solids flow and inlet solid temperature on the moisture content and solid temperature. An increase of gas temperature induced faster drying. As the particle diameter was increased, the drying process slowed down. In these calculations, gas velocity, dry solids flow and solid temperature had essentially no effect on the drying process. In order to make the model such a useful tool for process exploration and optimisation of this type of dryer, further validation with other materials is required.

Acknowledgements

The authors gratefully acknowledge the support provided by the Swedish International Development Cooperation Agency (Sida). A. Picado also acknowledges PixelMK, Inc., Nicaragua for providing the digitalisation of the experimental data.

Nomenclature

a_s	Specific area per unit bed volume	(m^2 m^{-3})
B	Dryer width	(m)
D	Mass transport coefficient	(m^2 s^{-1})
D_h	Thermal diffusivity	(m^2 s^{-1})
F	Mass flow per cross-section, dry basis	(kg m^{-2} s^{-1})
G_g	Molar evaporation flux	(kmol m^{-2} s^{-1})
h	Heat transfer coefficient	(W m^{-2} K^{-1})
H_b	Bed height	(m)
I	Enthalpy per unit mass, dry basis	(J kg^{-1})
k	Thermal conductivity	(W m^{-1} K^{-1})
k_m	Mass transfer coefficient	(kmol m^{-2} s^{-1})
L	Dryer length	(m)
M	Molecular weight of the moisture	(kg $kmol^{-1}$)
q	Heat flux	(J m^{-2} s^{-1})
r	Radial coordinate	(m)
S	Flow of dry solids	(kg s^{-1})
t	Time	(s)
T	Temperature	(K)
u	Transformed and dimensionless moisture content	(-)
u_g	Gas velocity	(m s^{-1})
V	Flow of dry gas	(kg s^{-1})
v	Forward bed velocity	(m s^{-1})
X	Solid moisture content, dry basis	(kg kg^{-1})
y	Molar fraction in the gas phase	(kmol $kmol^{-1}$)
Y	Gas humidity, dry basis	(kg kg^{-1})

z	Distance along the length of the bed	(m)

Greek Letters

δ	Particle radius	(m)
ε	Porosity	(-)
Θ	Transformed and dimensionless temperature	(-)
λ	Latent heat of vaporisation	(J kmol^{-1})
ν_h	Roots related to heat transfer	(-)
ν_m	Roots related to mass transfer	(-)
ρ	Density	(kg m^{-3})

Subscripts

b	Bed	*s*	Solid
e	Exit	*t*	Total
eff	Effective value	δ	Interface
g	Gas	∞	Gas bulk
p	Particle	0	Inlet

References

Baker, C.G.J., Lababidi, H.M.S. (2010). *An improved model of plug-flow fluidized bed dryers with an emphasis on energy conservation*. Drying Technology 28, 730-741.

Bizmark, N., Mostoufi, N., Sotudeh-Gharebagh, R., Ehsani, H. (2010). *Sequential modeling of fluidized bed paddy dryer*. Journal of Food Engineering 101, 303-308.

Daud, W.R.W. (2007). *A cross-flow model for continuous plug flow fluidized-bed cross-flow dryers*. Drying Technology 25, 1229-1235.

Daud, W.R.W. (2008). *Fluidized bed dryers-recent advances*. Advanced Powder Technology 19, 403-418.

Hacihafizoglu, O., Cihan, A., Kahveci, K. (2008). *Mathematical modelling of drying of thin layer rough rice*. Food and Bioproducts Processing 86, 268-275.

Izadifar, M., Mowla, D. (2003). *Simulation of a cross-flow continuous fluidized bed dryer for paddy rice*. Journal of Food Engineering 58, 325-329.

Khanali, M., Rafiee, S., Jafari, A., Hashemabadi, S.H. (2013). *Experimental investigation and modeling of plug-flow fluidized bed drying under steady-state conditions*. Drying Technology 31, 414-432.

Khanali, M., Rafiee, S., Jafari, A. (2014). *Numerical simulation and experimental investigation of plug-flow fluidized bed drying under dynamic conditions*. Journal of Food Engineering 137, 64-75.

Mujumdar, A.S. (2007). *Handbook of Industrial Drying*, third ed. CRC Press, Boca Raton, FL.

Park, K.J., Brod, F.P.R., de Oliveira, R.A. (2006). *Mass transfer and drying in vibro-fluidized beds-a review*. Engenharia Agrícola 26, 840-855.

Pfost, H.B., Maurer, S.G., Chung, D.S., Milliken, G.A. (1976). *Summarizing and reporting equilibrium moisture data for grains*. In: Winter Meeting of the American Society of Agricultural Engineers (ASAE); Chicago, USA.

Picado, A., Martínez, J. (2012). *Mathematical modeling of a continuous vibrating fluidized bed dryer for grain*. Drying Technology 30, 1469-1481.

Saravacos, G.D., Maroulis, Z.B. (2001). *Transport Properties of Foods*. Marcel Dekker, New York.

Steffe, J.F., Singh, R.P. (1982). *Diffusion coefficients for predicting rice drying behavior*. Journal of Agricultural Engineering Research 27, 489-493.

Wanjari, A.N., Thorat, B.N., Baker, C.G.J., Mujumdar, A.S. (2006). *Design and modeling of plug flow fluid bed dryers*. Drying Technology 24, 147-157.

Yang, W.C. (2003). *Handbook of Fluidization and Fluid-Particles Systems*. Marcel Dekker, New York.